HIGH PRESSURE PHASE TRANSFORMATION IN SINGLE CRYSTAL SILICON DURING DUCTILE REGIME DIAMOND TURNING

R. G. Jasinevicius
Departamento de Engenharia Mecânica - E.E.S.C. - USP, C. P. 359 CEP 13560-970 São Carlos - São Paulo - Brazil
e-mail: renatogj@sc.usp.br

P. S. Pizani
Departamento de Física - Universidade Federal de São Carlos - C.P. 676, CEP 13 565-905 São Carlos - SP - Brazil

Abstract. *Single point diamond turning of monocrystalline semiconductors is an important field of research within brittle materials machining. Monocrystalline silicon sample with (100) orientation was diamond turned under different cutting conditions (feed rate and depth of cut). Micro Raman spectroscopy and Atomic Force Microcscopy were used to assess structural alterations and surface finish of the samples diamond turned under ductile and brittle mode. It was found that silicon undergone a phase transformation when machined in the ductile mode. This phase transformation is evidenced by means of an amorphous phase surface layer probed by Raman scattering after machining. Compressive residual stresses were also estimated in the machined surface and it was observed that it decreases with the increase in the feed rate and depth of cut. This behavior was attributed to the formation of subsurface cracks when the feed rate was higher or equal to 2.5 μm/rev. The surface roughness was observed to vary with the feed rate and the depth of cut. The increase of surface roughness was influenced by microcracks formation when the feed rate reaches 5.0 μm/rev. Furthermore, high pressure phase transformation induced by the tool/material interaction and responsible by the ductile response of this typical brittle material will be discussed based upon the Raman spectra presented. The application of this machining technology finds a wide range of high quality components. For example, the generation of micrometer range channel for microfluidic devices as well as microlenses used in the infrared spectrum range.*

Keywords: Phase transformation, semiconductor crystals, ductile-to-brittle transition, diamond tool, ultraprecision

1. Introduction

Monocrystalline semiconductors are normally considered to be fragile and exhibit brittle response under conventional machining conditions. Furthermore, under particular critical conditions of depth and/or thickness of cut, it is possible to achieve the ductile mode material removal so as to generate a crack free surface. Plastic deformation during machining of crystalline brittle materials occurs by shear involving mechanisms of slip system activation and dislocation movement. Although it is well established that monocrystalline silicon exhibits limited dislocation mobility and, consequently, brittle behavior below 650 °C (Suzuki and Ohmura, 1996), the anomalous plastic behavior of silicon during machining experiments at room temperature has prompted new researches on this subject.

Results from high hydrostatic pressure (Minomura and Drickamer, 1962; Jameison, 1963), microindentation (Clarke et al., 1988; Gridneva, Milman and Trefilov, 1972; Cahn, 1992; Callahan and Morris, 1992) and microscratching (Minowa and Sumino, 1992; Morris and Callahan, 1994) experiments have demonstrated that diamond-cubic silicon transforms to the denser metallic β-tin structure at room temperature. Upon release of the pressure, a reversion to an amorphous semiconductor phase, with a cubic structure has been reported (Hu et al. 1988). Based on these facts, new hypotheses were proposed in the debate on the mechanism responsible for material removal in ductile regime diamond turning of semiconductor crystals. According to some results reported, it has been asserted that the ductile behavior has its origin attributed to this phase transformation induced by pressure/stress (Morris et al. 1995). Cross-section studies carried out on a surface after diamond turning of silicon (Shibata et al. 1994; 1996) indicates an amorphous phase in the outer most surface, providing support to this hypothesis of phase transformation. However, nothing was mentioned about the presence of crystalline phase immersed in an amorphous media in silicon. This fact can be important for optical fabrication from semiconductor crystals by means of mechanical grinding since this amorphous surface phase has to be considered as a barrier layer with a different refractive index from that of the substrate (Puttick et al., 1995).

Raman scattering can be considered a powerful characterization technique to evidence structural alteration in semicondutors materials because the vibrational spectrum of the material is greatly influenced by disorder and residual strains. These lead to changes in phonon frequencies, broadening of Raman peaks and breakdown of Raman selection rules (Loudon, 1964). For bulk crystalline Si (c-Si), the triple degenerate optical phonons display in the first-order Raman spectrum one sharp peak at 521 cm^{-1}. Due to the positive phonon deformation potentials of Si, compressive (tensile) strains lead to a positive (or negative) frequency shifts. On the other hand, due to the loss of phonon correlation length and the consequent breakdown of the q = 0 Raman selection rules (q is the phonon wave vector), disorder effects can lead to an asymmetric broadening and shifting of Raman peaks compatible to the dispersion relation of the material (Richter, Wang and Ley, 1981). In the silicon case, the frequency and asymmetry point to lower values because the

dispersion relationship presents decreasing optical frequencies, increasing phonon wave vectors. At maximum disorder (amorphous material, a-Si), the first-order Raman spectrum reflects the phonon density of states: it presents two broad bands centered at about 100 cm^{-1} (acoustic band) and 470 cm^{-1} (optical band) (Zwick and Carles, 1993).

Recently, new information has been added to discussion on the multiple phase found in silicon after mechanical deformation by microindentation with spherical indenter. The microstructure of transformed materials after cyclic microindentations, probed by Raman spectroscopy and cross-section transmission electron microscopy, consisted of specific phases of silicon which were formed in the second and subsequent indentation cycles under low loads (Bradby et al., 2000; Zarudi, Zhou and Zhang, 2003). An increase of the maximum load causes changes of subsequent indentation cycles of the phase transformation events to occur earlier on both loading and unloading (Zarudi, Zhang and Swain, 2003a). It was also reported that when the maximum load increases a crystalline phase of high pressure of body centered-cubic (named Si-III) and rhombohedral (Si-XII) can appear (Zarudi, Zhang and Swain, 2003b). Furthermore, different amorphous structures have been induced in monocrystalline silicon by high pressure in indentation and polishing (Zarudi et al. 2004). Transmission electron microscopy and nanodiffraction study of the indentations and polished samples showed that the structures of silicon formed at slow and fast loading/unloading rates are dissimilar and inherit the nearest-neighbor distance of the crystal which are formed (idem). These results are concerned with spherical indenters. Gogotsi and collaborators have also made interesting finding in this area using nanoindentation with Berkovich indenter (Ge, Domnich and Gogotsi, 2003, 2004). The authors proposed that a mechanism of dislocation-induced lattice rotation that leads to phase transition and distortion-induced amorphization during nanoindentation. Further more they used Raman spectroscopy and transmission electron microscopy to investigate the temperature effects on the stability of metastable silicon phases (Si-III and Si-XII) produced by nanoindentation. It was found that the thickness of the specimen beneath the residual imprint plays an important role in the phase transformation sequence during heating up to 200 °C (Ge, Domnich and Gogotsi , 2004).

Gogotsi et al. (2001) probing wear debris generated by scratching silicon with indenters of different geometries also detected policrystalinity. Besides amorphous silicon, they found Si-III, Si-XII and Si-IV (26). This is an important finding since during scratching there is a dynamic component which is similar to machining process. More recently, Zarudi, Nguyen and Zhang (2005) have shown that the size of the amorphous transformation zone and the depth of slip penetration in sample subsurface were mainly dependent on the stress field applied in scratching monocrystalline silicon. In this paper they reported an investigation on the effect of temperature and stress on plastic deformation in scratching by using dry air, coolant, and liquid nitrogen. The influence of the temperature variation to -196 °C was surprisingly small and the low temperature did not suppress the phase transformation and dislocation activity (idem).

Despite of all effort addressed to the investigation of the effects of diamond turning upon the machined surface, there still some aspects to be investigated. The ductile mode envolved in material removal may occur along with brittle mode and the surface is still damage free. This aspect will be discussed in this paper.

In this work, an original (micro)-Raman investigation of single point diamond turned monocrystalline silicon (100) oriented samples machined in ductile and brittle modes is presented. All measurements were performed at room temperature, with special care taken to avoid overheating the samples. Transmission Electron Microscopy (TEM) cross-section view analyses were also carried out after machining in order to characterize the structural alteration in the subsurface of the machined samples.

2. Experimental Procedure

Single-point diamond turning tests were carried out on a commercially available ultraprecision diamond turning machine, the Aspheric Surface Generator Rank Pneumo ASG 2500. Facing cuts were performed on silicon substrates (10 mm x 10 mm). A single crystal p-type Si (100) surface orientation sample was used in this study.

The cutting fluid used was synthetic water-soluble oil with the purpose of cooling and lubrication. This fluid was continuously mist sprayed onto the workpiece during machining. Round nose single crystal diamond tool geometry (Contour Fine Tooling®) was used. Only new diamond tools were used in the cutting tests. Table 1 describes the experimental conditions and tool geometries used in the cutting tests.

A specimen was machined for each combination of cutting parameters, i.e., feed rate and depth of cut, and the microtopography and morphology of the surface generated inspected by means of AFM. The atomic force microscope (AFM) was a Digital Nanoscope IIIa. It was operated with a standard 50-60° conical silicon nitride stylus of 5 nm radius tip, with cantilever spring constant of ~ 0.06 N/m. Conventional contact mode was employed where the stylus is scanned raster style over, and in contact with the surface with contact forces of typically 10-100 nN. For the characterization of the examined diamond turned surfaces it was decided to use Ra and Rmax (Rt), representing the average and a maximum amplitude value of the surface roughness. The inspection process consisted of measuring the surface roughness and obtaining images of the surface in order to observe the reproduction fidelity of the tool edge profile into the surface cut grooves.

The Raman measurements are performed using an U1000 Jobin-Yvon spectrometer to probe the depth profile of disorder effects, 514.5 nm line of an argon ion laser was used. For this line, the penetration depth is about 340 nm for c-Si. The laser power was kept low in about 200 mW, in order to avoid heating effects and cylindrical lens was used. For amorphous silicon (a-Si), the optical absorption coefficient can reach one order of magnitude higher, leading to

penetration depths of about tenths of nanometers, depending on the degree of amorphization (Apnes and Stuna, 1983; Carlson and Wronski, 1979).

A Transmission Electron Microscope, operated at 200 kV was used to conduct the observation of chips and surface. The chips observed were those left on the machined surface after the cutting tests. The silicon chips were suspended in isopropyl alcohol, and the mixture was then deposited onto a copper TEM grid (Formvar support or lacey carbon film). The silicon machined sample was cut into 2 mm^2 squares and lapped, polished with 5 and 1 μm SiC abrasive from the unmachined surface to a thickness of < 50 μm. The sample was then affixed to a copper-slotted TEM grid using epoxy and dimpled via argon ion milling to provide an electron-transparent central area.

Table 1 - Tool geometry and dimensions used in the cutting tests.

Tool Specifications	Dimensions
Tool material	Single crystal diamond
Tool nose radius (mm)	0.635
Rake angle	–25°
Clearance angle	12°
Feed rate (μm/rev)	1.0, 1.5 , 2.0, 2.5, 5.0
Depth of cut (μm)	0.1, 1.0, 5.0, 10

3. Results and Discussion

The results of surface finish showed that the increase in feed rate presented the expected effect, i.e., the increase in surface roughness. However, this change was not much pronounced as can be seen in Fig. 1. Fig. 1 shows 3-D images of the micro-roughness of the silicon surfaces machined with different feed rate conditions. R_{max} shows some difference with the increase in the feed rate condition. The morphology of the cutting grooves in all images shows equally spaced tooling marks according to the feed rate condition applied. No sign of cutting edge defect is found within the primary surface roughness structure. Figure 1 e) shows the tridimension image of the surface generated with the highet feed rate i.e., 5 μm/rev. Although a smooth surface finish is presented it is worth mentioning that the surface does present microcracks. Figure 1 also shows the average surface roughness values Ra of the machined surfaces. The roughness R_a did not show a significant variation and is almost constant around 2 nm. This average surface roughness is within the range required for optical parts used with infrared light ($Ra < 0.03 \ \mu m$).

There is an interesting aspect which was found for the sample machined with different depths of cut. A decrease was observed in surface micro-roughness Rmax. This tendency can be observed in Fig.2.. A possible explanation for this may be attributed to a more prominent spring back of the surface vicinity due to the back transformation to the amorphous phase occurred during machining. It is generally accepted that at pressure of 11-12.5 GPa, silicon crystal with diamond cubic form transforms to the denser β-tin structure with 22% reduction in volume. When the pressure is withdraw, this metallic phase undergoes another phase change to a bcc structure with an intermediate density between the crystal and the metallic phase; the unit cell volume is some 8% denser than the silicon crystal phase. In this case, this may be promoting a size effect as a function of the increase in depth of cut.

Micro Raman spectroscopy was also applied to assess the surface integrity and estimation of residual stresses within the surface induced by machining process. The Raman spectra obtained under different feed rate conditions is shown in Figure 3 It is likely to infer from both spectra presented in Fig. 3 that the crystal peak shift from the characteristic cubic diamond structure centered in 521.6 cm^{-1}. This means that the machined surface is under residual stress. The value of this stress canb be estimated by the formula proposed by Weinstein & Piermarini (1975):

$$\varpi = \varpi_0 + 5.2 \ P \ (GPa) \qquad (1)$$

where ϖ is the real position of the characteristic crystalline peak, ϖ_0 is the characteristic peak of cubic diamond structure of silicon (521.6 cm^{-1}) and P is the stress within the machined surface in GPa. The values of the residual stresses estimated by means of this formula shown in Table 2. The Raman spectra shift upward with the decrease of the feed rate. This trend shows that the residual stress is compressive. In addition, the values obtained show very interesting information: the residual stress increase with the feed rate up until 2.0 μm/rev and then decreases with the subsequent passes with 2.0 μm/rev, 2.5 μm/rev and 5.0 μm/rev, respectively. The reason why the residual stress decrease can be explained with transmission electron microscopy results shown in Figure 4. Figure 4a) shows cross-section view of the sample machined with 1 mm/rev feed rate, no sign of microcracks are observed to be formed in the subsurface. On the

other hand, figure 4b shows the sample cut with 2.5 mm/rev feedrate where it is observed the formation of subsurface cracks. The average measured residual stress is much lower than that in the crack free zone because the elastic strain is released by cracking, as already observed in Table 2.

a) f = 1.0 μm/rev R_{max} = 38.25 nm, Ra = 2.5 nm   a) f = 1.5 μm/rev R_{max} = 37.13 nm, Ra = 2.3 nm

c) f = 2.0 μm/rev R_{max} = 38,3 nm, Ra = 2.3 nm   d) f = 2.5 μm/rev R_{max} = 40.9 nm, Ra = 2.1 nm

e) f = 5.0 μm/rev R_{max} = 39.25 nm, Ra = 2.1 nm
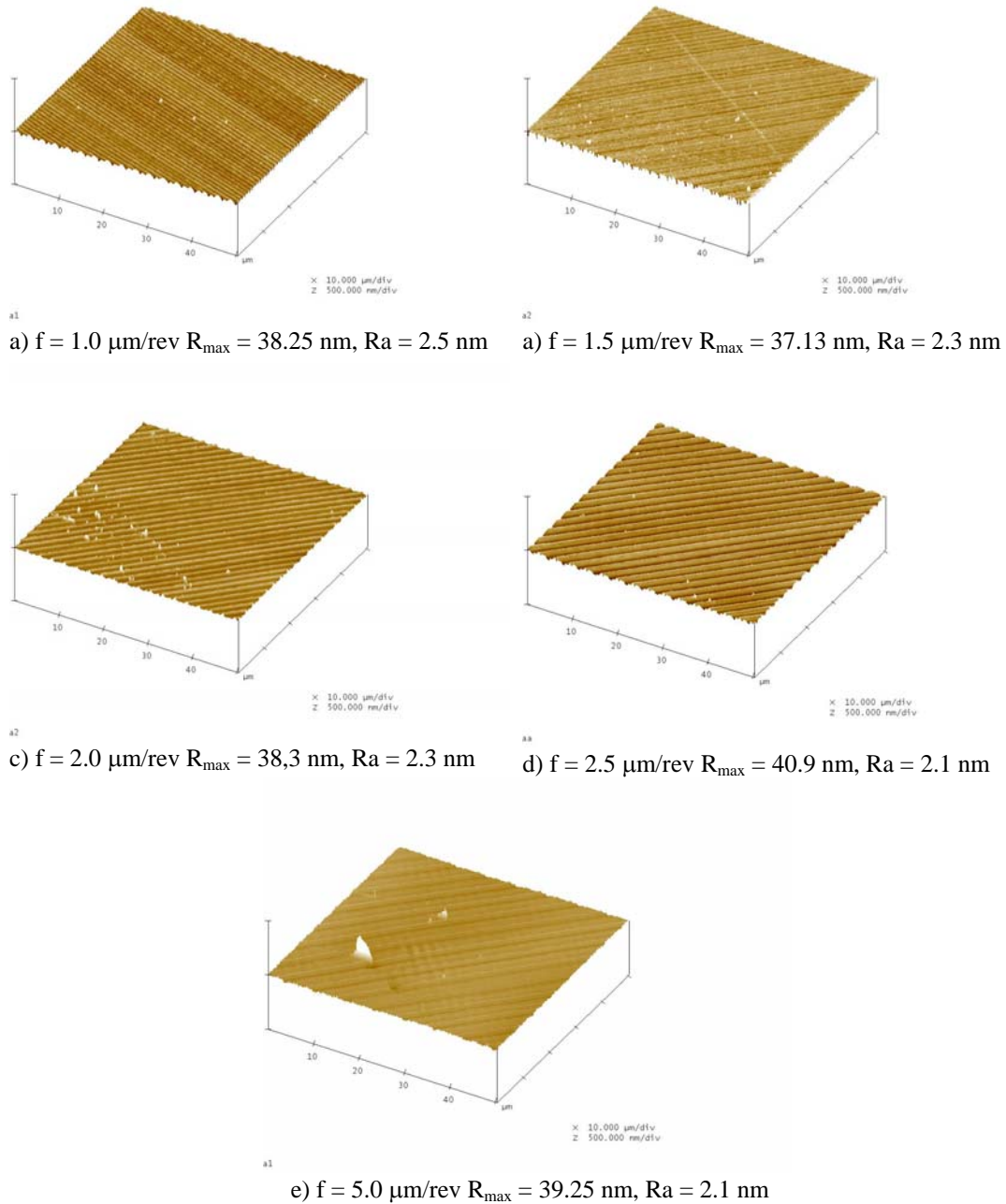
Figure 1. 3-D images of micro-roughness difference for the machined samples cut with different feed rates: a) 1.0 μm/rev, b) 1.5μm/rev, c) 2.5 μm/rev, and d) 5.0 μm/rev.
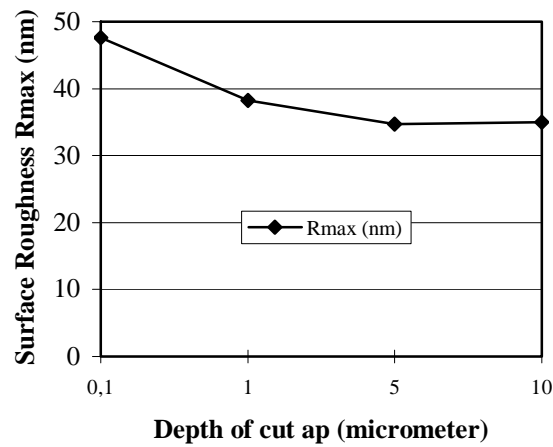
Figure 2. Rmax value as function of depth of cut.
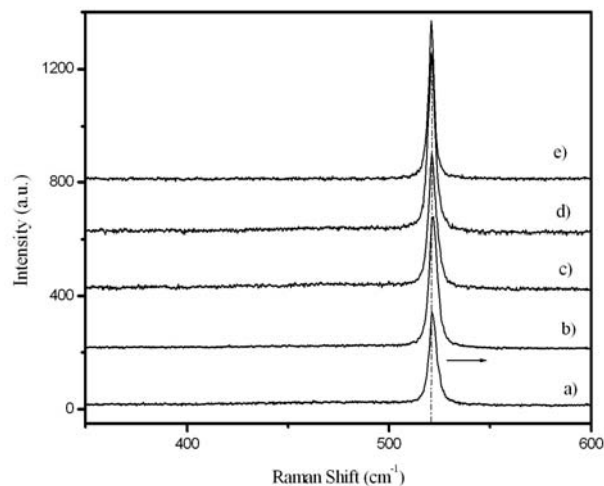
Figure 3. Raman spectra of the machined surface under different feed rate: a) 1.0 μm/rev; b) 1.5 μm/rev; c) 2.0 μm/rev; d) 2.5 μm/rev; e) 5.0 μm/rev.

Table 2. Residual stress values estimated with feed rate variation.

Feed rate (μm/rev)	Residual stress (MPa)
1,0	+13.5
1.5	+17.2
2.0	+8.0
2.5	+2
5.0	0

Table 3 show the residual stress values estimated for depth of cut variation. In this case, the residual stress decreases with the increase in depth of cut. This can be explained by the same manner used to explain the former case. The stress distribution will tend to be lower in the tool-workpiece interface with the increase in depth of cut since the width of cut is larger. Since silicon is a brittle material, instead of sustaining a larger plastic deformation volume the subsurface generates a larger number of defects such as dislocation, and micro cracks are likely to be formed. Consequently, once cracks form, the local strains around the cracks relax, leading to strong stress variation.

Table 3. Residual stress values estimated with feed rate variation.

Depth of cut (μm)	Residual stress (MPa)
0.1	+11
1.0	+10
5.0	+8.0
10.0	+6.3
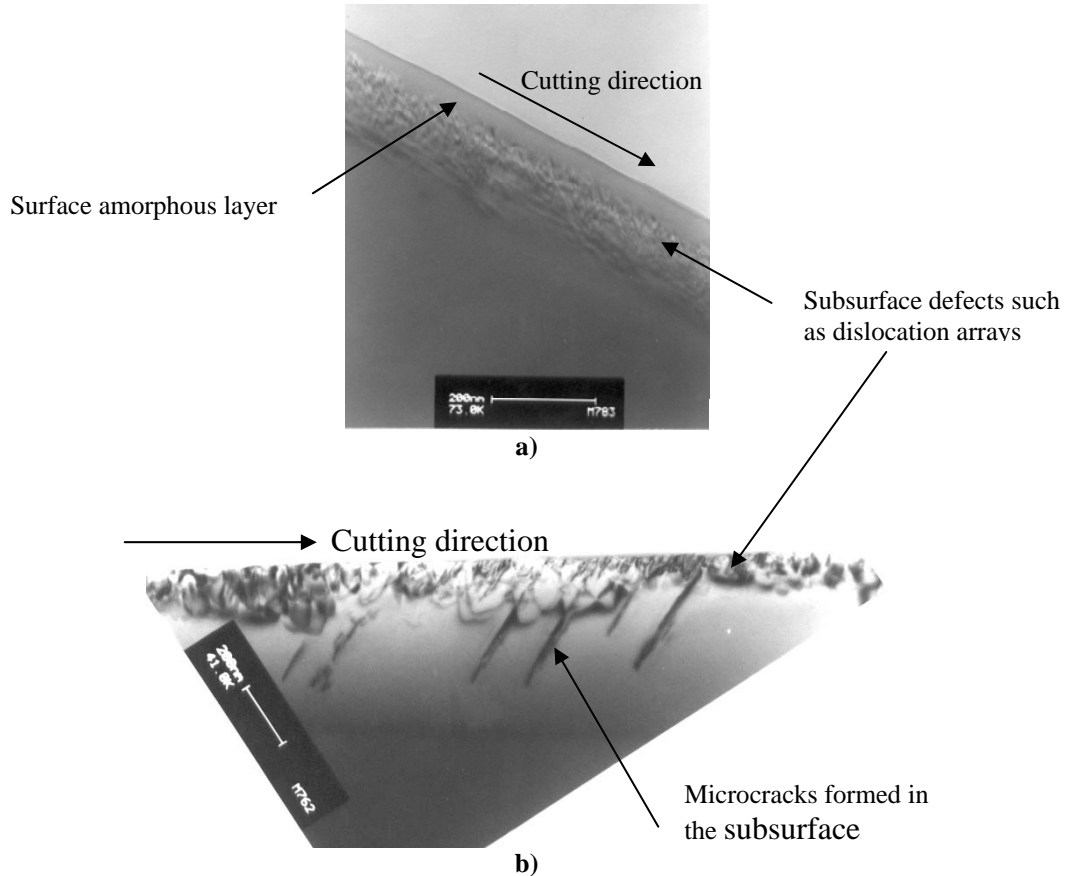
Figure 4. Cross-section view made by Transmission electron microscopy of silicon samples machined under 2 different cutting conditions: a) f = 1.0 μm/rev and; b) f=2.5 μm/rev.

Ductile regime machining with sharp tools may be used as an alternative for marking (engraving) semiconductor wafers, which is currently done using lasers. It can also produce deep grooves in Si wafers that are required for MEMS or microfluidic devices, which are finding increasing application in analytical and biomedical systems (Gogotsi et al. 2001). Conventional methods for fabricating microfluidic devices have centred on etching channels in glass and silicon (Richter et al., 1999; Stjernstrom and Roeraade, 1998). By applying the ductile cutting techniques discussed in this paper, we can employ a sharp tool to produce complicated microfluidic channels without introducing brittle fracture. This method is not dependent on the crystal orientation, and channel shapes other than that permitted by the selective etchant and crystal structure can be produced. Slight etching may be used after this method is employed to remove the metastable phases and decrease residual stresses.

4. Conclusions

Pressure-induced metallization has been shown to play a key role in the process of ductile regime machining of semiconductor crystal. A combination of diamond turning tests, microscopy techniques (TEM and AFM) and Raman spectroscopy analysis can be used to optimize and monitor ductile regime machining of semiconductors. Raman

spectroscopy shows the presence of metastable silicon phase (amorphous silicon) surfaces produced on monocrystalline silicon single point diamond tool.

The mechanism of material removal during scratching, using a sharp tool, involves ductile removal of the metallic phase to a critical depth of cut when microfracture starts in the subsusrface. The onset of susbsurface cracks seems to depends on feed rate and depth of cut. Microfracture can be suppressed by controlling the both parameters.The residual stresses decrease with the feed rate and depth of cut increase. The highest residual stress is shown to exist with low feed rate, 1.5 µm/rev, a is in the range of 17 MPa.

5. Acknowledgements

6. References

Aspnes D E, Studna AA. Dielectric Functions and Optical-Parameters of Si, Ge, GaP, GaAs, GaSb, InP, InAs, and Insb from 1.5 To 6.0 Ev. *Physical Review B.* 1983; 27(2):985-1009.

Bradby JE, Williams JS, Wong-Leung J, Swain MV, Munroe P. Mechanical deformation in silicon by micro-indentation. *Journal of Materials Research*, 2001; 16(5):1500-1507.

Cahn RW. Metallic solid silicon. *Nature.* 1992; 357(6380):645-646

Callahan DL, Morris JC. Extent of phase transformations in SI hardness indentations . *Journal of Materials Research.* 1992; 7(7):1614-1617.

Carlson DE, Wronski CR. *Topics in Applied Physics,* Vol. 36, edited by M. H. Brodsky (Springer-Verlag), New York, 1979.

Clarke D.R., Kroll M.C., Kirchner P.D., Cook R.F., Hockey B.J. Amorphization and conductivity of Si and Ge during indentation. *Physical Review Letter.,* 1988; 60(21): 2156-2159.

Ge D, Domnich V, Gogotsi Y. *Journal of Applied Physics*, High-resolution transmission electron microscopy study of metastable silicon phases produced by nanoindentation. 2003; 93(5):2418-2423.

Ge D, Dominich V, Gogotsi Y. *Journal of Applied Physics,* Thermal stability of metastable silicon phases produced by nanoindentation. 2004; 95 (5): 2725-2731.

Gogotsi Y, Zhou G, Ku SS, Cetinkunt S. Raman microspectroscopy analysis of pressure-induced metallization in scratching of silicon *Semiconductors Science and Technology*, 2001; 16(5):345-352.

Gridneva IV, Milman YV, Trefilov, M. Phase transformation in diamond-structure crystals during **hardness** measurements. *Physics Status Solidi A.* 1972; 14(1): 177-182.

Hu, J.Z., Markle L.D., Menoni C.S., Spain I.L. Crystal data for high-pressure phases of silicon. *Physical Review B.* 1986; 34(7):4679-4684.

Jameison JC. Crystal sutructures at high pressures of metallic modifications of Si and Ge. *Science.* 1963; 139(2):762-764.

Loudon R. Raman Effect in Crystals *Advanced Phys*ics , Raman Effect In Crystals 1964; 13(52):423-428.

Minomura S, Drickamer, H.G., *Journal of Physics and Chemistry of Solids.* 1962; 23(5): 451-462.

Minowa K, Sumino K. Stress-Induced amorphization of a silicon crystal by mechanical scratching. *Physical Review Letters.* 1992; 69(2):320-322.

Morris JC, Callaham DL. Origins of microplasticity in low-load scratching of silicon. *Journal of Materials Research.* 1994; 9(11):2907-2913. Falta titulo do paper.

Morris JC, Callaham DL, Kulik J, Patten JA, Scattergood RO. Origins of the ductile regime in single-point diamond turning of semiconductors *Journal of the American Ceramic Society.* 1995; 78(8):2015-2020.

Pharr GM, Oliver WC, Harding DS. New evidence for pressure induced phase transformation owing indentation of silicon. *Journal of Materials Research.* 1991; 6(6):1129-1130.

Puttick KE, Whitmore LC, Gee AE, Chao CL. Energy Scaling transitions in machining of silicon by diamond. *Tribology International*, 1995; 28(6):349-355

Richter H.Z, Wang P., Ley L. The One Phonon Raman-Spectrum in Microcrystalline Silicon. *Solid State Communications*, 1981; 39(5): 625-629.

Richter K, Orfert M, Howitz S and Thierbach S 1999 Deep plasma silicon etch for microfluidic applications *Surf. Coatings Technol.* **119,** 461-467.

Shibata T, Ono A, Kurihara K, Makino E, Ikeda M. X., Cross-section transmission electron-microscope observations of diamond-turned single-crystal Si surfaces. *Applied Physics Letters.* 1994; 65(20):2553-2555.

Shibata T, Fujii S, Makino E, Ikeda M. Ductile-regime turning mechanism of single crystal Si. *Precision Engineering.*, 1996; 18(2/3):129-137.

Stjernstrom M and Roeraade J 1998 Method for fabrication of microfluidic systems in glass *J. Micromech. Microeng.* 8 (1):33-38.

Suzuki T, Ohmura, T. Ultramicroindentation of silicon at elevated temperatures. *Philosophical Magazine A*. 1996; 74(5): 1073-1084.

Zarudi I, Zou J, Zhang LC. Microstructures of phases in indented silicon: A high resolution characterization. *Applied Physics Letters;* 2003a; 82(6):874-876

Zarudi I, Zhang LC, Swain MV. Behavior of monocrystalline silicon under cyclic microindentations with a spherical indenter. *Applied Physics Letters*. 2003b; 82(7):1027-1029.

Zarudi I, Zhang LC, Swain MV. Microstructure evolution in monocrystalline silicon in cyclic microindentations. *Journal of Materials Research*., 2003c; 18(4):758-761.

Zarudi I, Zou J, McBride W, Zhang LC. Amorphous structures induced in monocrystalline silicon by mechanical loading. *Applied Physics Letters*, 2004; 85(6):932-934.

Zwick A, Carles R. Multiple-Order Raman-Scattering In Crystalline And Amorphous-Silicon. *Physical Review* B .1993; 48(9):6024-6032.

Zarudi I, Nguyen ., Zhang LC. *Applied Physics Letters,* Effect of temperature and stress on plastic deformation in monocrystalline silicon induced by scratching. 2005; 86(1): Art. No. 011922.